

Ru₃Pd₆Pt Nanocatalyst for the Oxygen Reduction in a PEM Fuel Cell

F. Leyva-Noyola, O. Solorza-Feria*

Depto. Química. Centro de Investigación y de Estudios Avanzados del IPN, A. Postal 14-740, C.P. 07360, México D.F., Mexico.

*E-mail: osolorza@cinvestav.mx

Received: 25 September 2012 / *Accepted:* 16 October 2012 / *Published:* 1 November 2012

Nanosized and highly dispersed on carbon black low platinum Ru₃Pd₆Pt catalyst, was synthesized by the reduction of RuCl₃, PdCl₂ and H₂PtCl₆ in ethylene glycol solution at 180°C, studied for the oxygen reduction reaction in acid media and in a single PEM fuel cell. XRD, SEM and TEM measurements were used to characterize the synthesized three metallic catalysts. Results conducted to nanocrystallites of 3-9 nm in average sizes with a spherical shape homogeneously and highly dispersed particles. Kinetic parameters were evaluated from steady state measurements with a rotating disk electrode (RDE) in a 0.5M H₂SO₄ solution at room temperature. The catalyst was tested as a cathode electrode in a single H₂/O₂ PEM fuel cell, achieving a power density of 175 mW cm⁻² at 0.40 V and 80°C.

Keywords: Polyol method; Ru₃Pd₆Pt; Oxygen reduction reaction; Electrocatalysts; PEM Fuel cells.

1. INTRODUCTION

Interest in clean energy generation has motivated thriving research on the synthesis and characterization of novel, stable and inexpensive electrocatalysts for the four-electron transfer process of the oxygen reduction reaction, ORR, to water formation [1-7]. The synthesis and characterization of nanostructured materials represent one of the major breakthroughs of the modern science, enabling materials of distinctive shape, size, structure, density and composition to be produced. However, reliable methodology of the fabrication of nanostructured materials remains as an area of active research. Polymer electrolyte membrane fuel cells, PEMFCs, are very attractive as energy efficient and environmentally friendly power sources for many applications including automotive transportation, stationary and portable power sources. However, to make PEMFC commercially viable several problems should be solved, where two of the main issues facing the development are the synthesis of efficient solid electrolyte membrane and to more effective catalysts than the scarce Pt for the oxygen

reduction reaction [8-10]. The design and production of stable catalytically active material require fundamental breakthrough on the chemical processes for the synthesis of different practical materials, pushes to meet high current density at low overpotential together with stability and durability for a long time. The ORR is a sluggish electrochemical reaction and leads to higher reduction overpotential, due to the fact that the oxygen-oxygen bond in the dioxygen molecule require higher bond dissociation energy. The synthesis and characterization of multi-metallic catalysts for the ORR have been a particular area of research, because it has been established that for the cathodic reaction, multi-metallic surface have superior activity than the obtained for a metallic alone [11, 12]. The enhanced activity is attributed to bifunctional effects where the catalytic properties of each element in the compound combine in a synergetic manner to yield a more active surface than each of the element alone. Historically, the synthesis methods for the catalysts preparation have involved high temperatures and relative high pressures; a long time for synthesis and organic solvents that requires extraction and purification steps. To date catalysts synthesis arises as promising as being able to finalize the process in a few minutes, achieving an efficient way which greatly reduces environmental impact. Because polyol process can transfer energy directly to the reactive species, the reactions can be carried out in shorter times than would normally be employing other methods [13-15].

In this work, the synthesis and characterization of a low platinum content Ru₃Pd₆Pt nanocatalyst synthesized *via* the polyol method is reported. Furthermore, ink-type thin film electrodes were prepared and the electrocatalytic studies were performed by cyclic voltammetry (CV) and rotating disk electrode (RDE). After the electrochemical analysis were carried out, the performance of the membrane electrode assembly (MEA) in a single polymer electrolyte membrane PEM fuel cell is also presented, using Ru₃Pd₆Pt nanocatalyst as a cathode electrode and Pt (E-Tek) as anode electrode.

2. EXPERIMENTAL

2.1 Electrocatalyst preparation

All reactants were used as received and without purification process. Nanosized and highly dispersed catalyst of Ru₃Pd₆Pt were synthesized by polyol process, by the reduction of the corresponding salts in a round-bottom flask. The RuCl₃ (Aldrich, 3.8 mM), PdCl₂ (Aldrich, 7.9 mM), H₂PtCl₆ (Aldrich, 1.5 mM) were added in 100 ml of ethylene glycol (Aldrich). The mixture in the flask was sonicated for five min, and then it was refluxed at 180 °C (0.03° s⁻¹) for 30 min, under vigorous stirring, maintaining the nitrogen flux above the solution. When heating the color of the solution was changed from dark brown to black, at the end of the reaction the solution was clear and dark particles was precipitated. Then the stirring was stopped and the product was cooled at room temperature. The reaction product was washed several times with tridistilled water and acetone (Aldrich) to remove the byproducts of the reaction and traces of the solvent. Afterwards the powders was dried at 60 °C for overnight and kept in a closed vessel. The products yield obtained was about 96%. The resulted dark-fine powder was used for physical characterization and electrochemical measurements.

2.2 Physical Characterization

X-ray diffraction was performed using a D8 Advance Diffractometer (Bruker) with monochromatic Cu K α radiation ($\lambda=1.54 \text{ \AA}$) in a measuring range of 35° to 90° of 2θ degree with a step width of $0.02^\circ \text{ min}^{-1}$. The spectra were analyzed with Topas Academic software to determine the average particle size and estimate a crystallinity degree. The particle shape was observed by scanning electron microscopy and transmission electron microscopy in a JEOL-2200FS operated at 200 kV equipped with energy-dispersive X-ray (EDX) spectroscopy used to obtain an average and local chemical compositions of the sample.

2.3 Electrochemical characterization

The configuration more commonly used was employ and consists of a double-compartment cell. The working electrode, a platinized titanium mesh as counter-electrode and the reference electrode was Hg/Hg₂SO₄/H₂SO₄ 0.5M (MSE = 0.68 V/NHE). Potentials are referred to NHE. An EG&G Princeton Applied Research (PAR mod 273A) potentiostat was used for the electrochemical experiments. CO stripping, cyclic voltammetry and rotating disk electrode measurements were conducted on a ink-type thin film catalysts deposited on a glassy carbon disk electrode (0.125 cm^2) mounted in an interchangeable RDE holder (Pine Instruments). The glassy carbon disk working electrode was prepared according to a method reported previously [16, 17]. A thin film was deposited from a solution prepared by adding $3.5 \mu\text{L}$ of a resulting suspension from a mixture of $40 \mu\text{L}$ of ethyl alcohol (spectroscopy grade, Aldrich) and $5 \mu\text{L}$ solution containing Nafion[®] (5 wt.%, Du Pont[®], 1000 EW) and 1 mg of dispersed catalyst at 26% on Vulcan[®] carbon. The estimated amount of catalyst on the glassy carbon electrode surface was about 0.164 mg cm^{-2} . The electrolyte was prepared from sulphuric acid (Merck, 97%) and ultra pure water (Millipore, $18 \text{ M}\Omega \text{ cm}$). The hydrodynamic experiments were recorded in the rotation rate range of 100–1600 rpm at 5 mV s^{-1} . During the ORR measurements an oxygen flux was maintained above the electrolyte surface. All the experiments were performed at room temperature (24°C).

For the CO stripping, the CO was adsorbed by flowing CO in nitrogen gas mixture at low flow for 5 minutes, while holding the electrode potential at 0.1 V, by keeping that potential at the same value for 15 minutes, while N₂ was employed to remove the CO traces from the solution. The potential was scanned from the starting potential to 0.05 V and then returned to 1.2 V. The sweep rate was 20 mV s^{-1} .

For the cyclic voltammetric study the solution was saturated with high purity nitrogen (99.997%, Infra) for 25 minutes and the potential was scanned from the open circuit potential to 0.05 V and then returned to 1.2 V for at least 50 cycles, at scan rate the 100 mV s^{-1} . After the solution was saturated with high purity oxygen (99.99%, Infra) the RDE experiments was performed at scan rate 5 mV s^{-1} .

2.4 Preparation and characterization of a membrane-electrode assembly (MEA)

The MEAs were tested with a commercial fuel cell system (CompuCell GT, Electrochem 890B) in a single cell with an effective electrode surface area of 5 cm^2 operated with H_2 and O_2 high purity at $100 \text{ cm}^3 \text{ min}^{-1}$. The humidification was fixed $5 \text{ }^\circ\text{C}$ above the cell temperature. The performance was measured under steady-state conditions from 25 to $80 \text{ }^\circ\text{C}$. A carbon cloth was used as gas diffusion layer in the cathode side and a commercially available Pt catalyst (1 mg , $20 \text{ wt}\%$ Pt/C, E-TEK) was used in the anode side. A cathodic catalytic ink were prepared sonicating a suspension formed by the $\text{Ru}_3\text{Pd}_6\text{Pt}$ electrocatalysts, Vulcan[®] carbon, Nafion[®] ionomer and ethanol. The MEA was prepared by spraying the corresponding catalyst ink onto the cathodic side of the Nafion[®] 115 (Du Pont[®]) used as a polymer electrolyte membrane, which was pretreated according to the procedure described in ref [18]. The catalyst loading at the cathode side was about 0.8 mg cm^{-2} . The MEA was prepared by hot-pressing the assembly at $120 \text{ }^\circ\text{C}$ and $11 \text{ kg}_f \text{ cm}^{-2}$ for 2 minutes. The input H_2 and O_2 flow rate were both 100 mL min^{-1} with 100% RH. The gas pressures were fixed at 30 psi for anode and cathode. The cell was activated at room temperature at the open circuit potential for 10 min and then at a constant voltage of 0.4 V for 10 min. This procedure was repeated for at least 12 cycles in order to enhance humidification and activation of the MEA. The activation process was carried out before the current-voltage curve measurements.

3. RESULTS AND DISCUSSION

3.1 Physical Characterization

X-ray diffraction pattern of $\text{Ru}_3\text{Pd}_6\text{Pt}$ synthesized by polyol method is shown in Fig. 1. The diffraction pattern shows at least six diffraction picks corresponding to the positive shifted face-centered cubic (fcc) crystal lattice of the hexagonal phase of palladium and platinum patterns nor to ruthenium reported on standards JCPDS card codes (Pd, 65-2867), (Pt, 65-2868), (Ru, 65-7646), respectively. Since, almost all the characteristics peaks are closed between themselves it is not possible to determine by XRD if it is a new phase formed as a result of the incorporation of all the three elements inside a crystalline structure. Although it is possible that the ruthenium nanometric were immersed in a lattice crystalline type fcc formed by Pd-Pt alloy [19]. The small peak observed at 43.8° could be associated to crystalline hexagonal Ru phase which probably appears as not alloyed or segregated particles. The XRD pattern was fitted using the academic Topas software to determine in some extent an average crystallite sizes. Results conducted to about 5 nm . The crystallinity percentage was determined by means of MDI Jade 5.0 software and results conducted to 65% $\text{Ru}_3\text{Pd}_6\text{Pt}$ electrocatalyst. Based on the above results, $\text{Ru}_3\text{Pd}_6\text{Pt}$ electrocatalyst can be described as the synthesized material presents a complex combination of amorphous and crystalline phase.

The SEM micrograph of the as-synthesized $\text{Ru}_3\text{Pd}_6\text{Pt}$ powders is shown in Fig. 2. SEM image shows small homogeneous agglomerated particles with spherical shape and less than 100 nm in size.

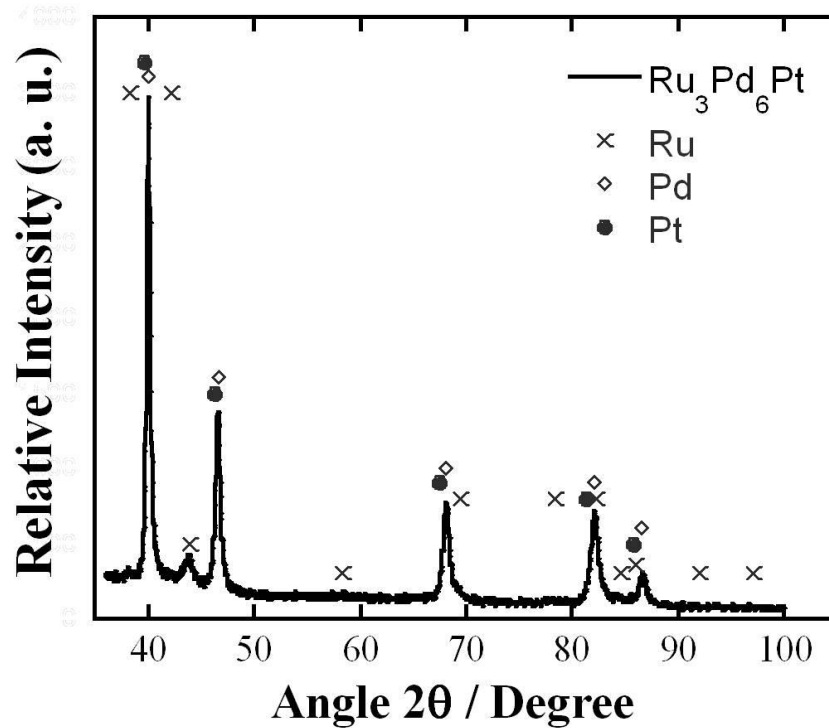


Figure 1. XRD spectra of the as-synthesized Ru₃Pd₆Pt catalyst.

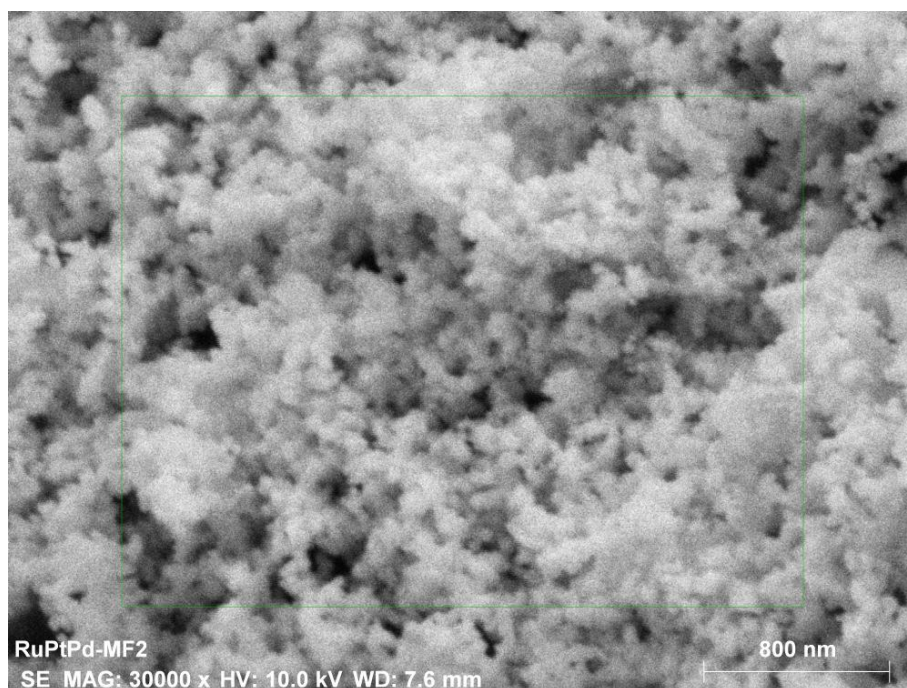


Figure 2. SEM image of the Ru₃Pd₆Pt catalyst powder.

Figure 3 shows the TEM images obtained in the as-synthesized Ru₃Pd₆Pt where the agglomerated spherical particles observed are constructed of small particles with a size distribution in the range of 3-9 nm, which is in agreement with results obtained from XRD data. The Fig. 3b shows a close-up image where it is possible to appreciate particles with a few nanometers in size. Fig. 3c shows the corresponding selected area of diffraction patterns from 3a were circles definite shiny points that is characteristic of a highly crystalline material, corresponding with that obtained with Jade software. Elemental average composition of the catalyst deduced from EDX is 33.13 at.% Ru, 56.06 at.% Pd and 10.79 at.% Pt, results which are in agreement with the estimated composition used for the catalyst preparation. Results suggest that the polyol process is a suitable method to synthesize three-metallic nanocatalyst.

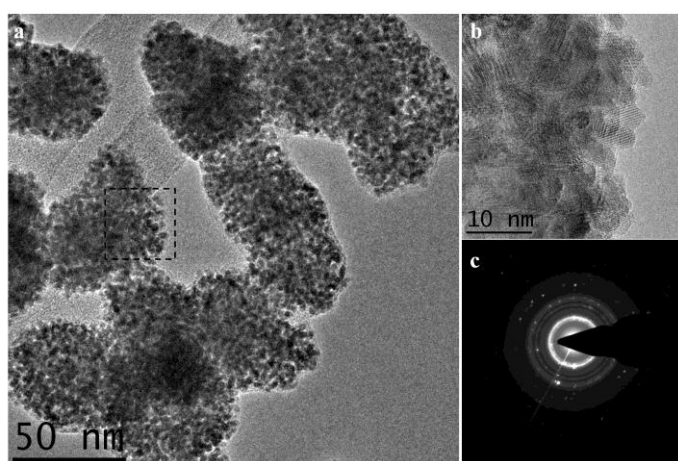


Figure 3. TEM image of a) Ru₃Pd₆Pt catalyst, b) close-up from the dotted black box and c) the electron diffraction pattern of the crystalline material.

3.2 Electrochemical characterization

The cyclic voltammograms of Ru₃Pd₆Pt nanocatalyst in N₂-saturated 0.5M H₂SO₄ before and after CO stripping, are shown in Fig. 4. Previously, the working electrode was subject to 30 cycles in the range of 0.05 V to 1.2 V/NHE to removed impurities and oxides from the electrode surface. The voltammograms show a typical feature of a hydrogen UPD region between 0.03 V and 0.30 V/NHE, followed by a double layer region and specific hydroxide adsorption-desorption peaks in the range of 0.60V to 1.00V/NHE. A CO stripping voltammetry applied to estimate an electrochemical surface area, EAS, in the material is showed in an inset of the Fig. 4, where continuous line is used as the base line. The EAS was calculated with eq. 1 [20]:

$$EAS = \frac{Q}{m_C Q_{RuPdPt,CO}} \quad (1)$$

where $Q_{RuPdPt} = 0.42 \text{ mC cm}^{-2}$ [21] is the charge associated with the formation of a CO monolayer in the test electrode surface, m_c the catalyst load, and Q the integrated area under the CO desorption peak. Value of $1.21 \pm 0.13 \text{ cm}^2$ where calculated from integrated curves and a roughness factor closed to 10 was deduced.

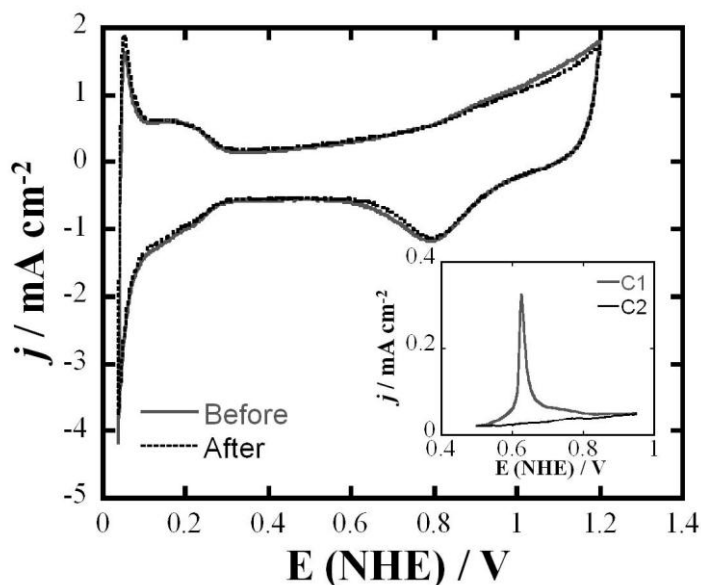


Figure 4. Cyclic Voltammograms of Ru_3Pd_6Pt catalyst in N_2 -saturated H_2SO_4 0.5M (gray line) and when applied the CO stripping technique (dotted line). Sweep rate 100 mV s^{-1} . Inset: CO stripping after CO_2 adsorption on Ru_3Pd_6Pt at 0.15 V/NHE . Sweep rate 20 mV s^{-1} at room temperature.

The potentiodynamic behavior of the Ru_3Pd_6Pt nanocatalyst in O_2 -saturated 0.5M H_2SO_4 at different rotation rates is shown in Fig. 5a. Three different potential regions are well defined: a diffusion-controlled region at potential bellow 0.70V/NHE followed by a diffusion-kinetic limited region between 0.70V and 0.80 V/NHE and a kinetic transfer region above 0.80V/NHE . Inset Fig 5b Koutecky-Levitch $1/j$ vs. $\omega^{1/2}$ plot was expressed by equations (2) and (3), without further need of additional terms [22-24]:

$$\frac{1}{j} = \frac{1}{j_k} + \frac{1}{j_D} \tag{2}$$

$$j_D = 0.2nFD^{2/3} C_{O_2} \nu^{-1/6} \omega^{1/2} \tag{3}$$

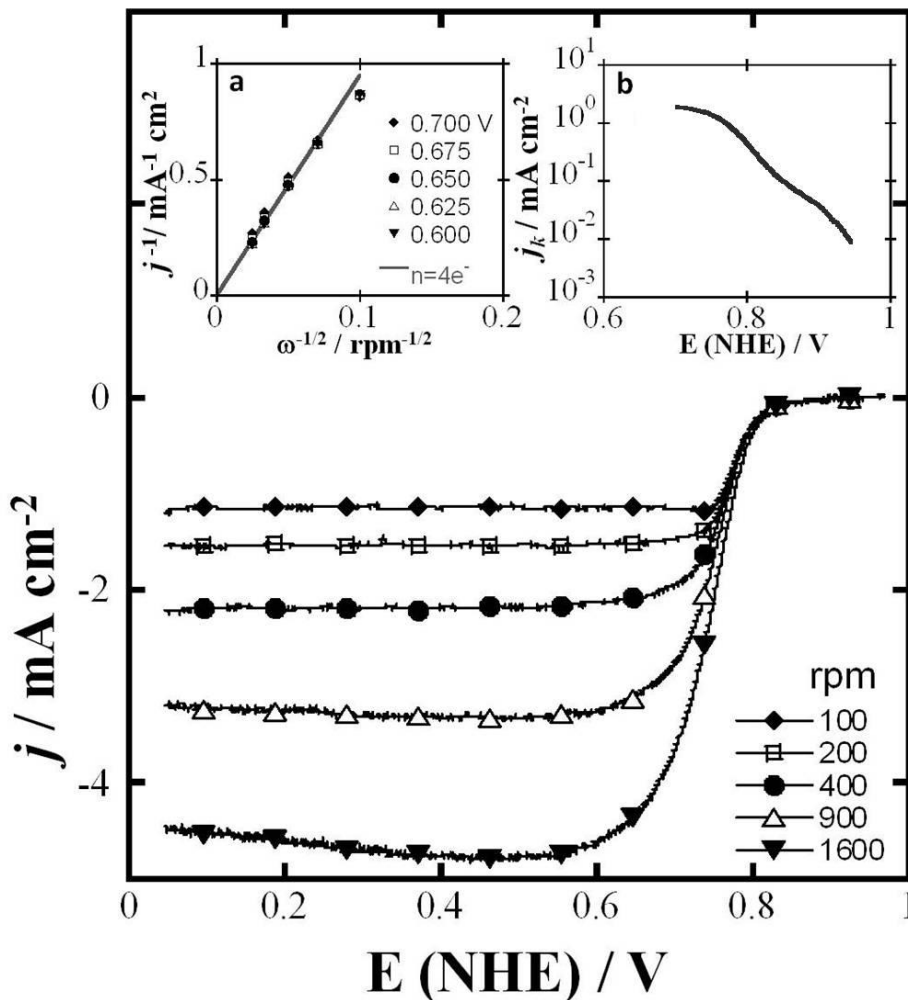


Figure 5. Steady-state polarization curves for the ORR in O₂ saturated H₂SO₄ 0.5 M on Ru₃Pd₆Pt catalyst. a) Koutecky-Levich plots at different electrode potentials and b) Mass transfer corrected Tafel plot where kinetic parameters were deduced.

Where j_k is the kinetic current density, j_D is diffusion limiting current density, n is the number of exchanged electrons, 0.2 is a constant used when ω is expressed in revolutions per minute, F is the Faraday constant (96485 C mol⁻¹), D is the diffusion coefficient of the molecular oxygen in 0.5M H₂SO₄ (1.4x10⁻⁵ cm²s⁻¹), ν is the kinematic viscosity (1x10⁻² cm²s⁻¹) and C_{O_2} is the concentration of molecular oxygen (1.1x10⁻⁶ mol cm⁻³) [25]. The theoretical plot for ORR, which corresponds to 4 electron transfer process, is shown in the same graph. The theoretical calculated slope for $n = 4e^-$ was $12.63 \times 10^{-2} \text{ mAcm}^{-2} \text{ rpm}^{-1/2}$, in accordance with experimental result of $11.97 \times 10^{-2} \text{ mAcm}^{-2} \text{ rpm}^{-1/2}$. The mass transfer corrected Tafel plot is shown in Fig. 5c, corresponding to the kinetic current, j_k , determined by equation (4) [24-27]:

$$j_k = \frac{j j_D}{j_D - j} \tag{4}$$

The kinetic parameters deduced from Fig 5c, at low overpotential was a Tafel slope of $b = 44.3 \pm 0.98 \text{ mV dec}^{-1}$, transfer coefficient $\alpha = 0.58 \pm 0.01$ and exchange current density $j_0 = 2.2 \pm 0.5 \times 10^{-5} \text{ mA cm}^{-2}$. From these results it can be estimated a first electron transfer rate determining step for the ORR on $\text{Ru}_3\text{Pd}_6\text{Pt}$ nanocatalyst, followed by a multi-electron charge transfer process to water formation, i.e., $\text{O}_2 + 4\text{H}^+ + 4\text{e}^- \rightarrow 2 \text{H}_2\text{O}$. But this assessment can only be demonstrated by the RRDE technique, which is now in route.

3.3 Polymer Electrolyte Fuel cell Performance

A Membrane-electrode assembly MEA was composed of $\text{Ru}_3\text{Pd}_6\text{Pt}$ cathode catalyst dispersed in Vulcan Carbon and deposited by aspersion onto Nafion 115 and commercial Pt (20wt%/C) (E-Tek) as anode electrode. Figure 6 shows the bell shape response of the single fuel cell performance at different temperatures for the MEA containing a catalyst loading of 0.64 mg cm^{-2} $\text{Ru}_3\text{Pd}_6\text{Pt}$ cathode catalyst at 40 wt %/C and $0.8 \text{ mg Pt (20 wt\%/C)}$ anode. An improvement of the MEA performance with an increase of the operating temperature was observed. The open circuit voltages were around 0.90 V at the operation temperature. The maximum performance expressed in power density obtained at 80°C and 30 psi of pressure with a flow rate of $100 \text{ cm}^3 \text{ min}^{-1}$ for both gases, was 175 mW cm^{-2} .

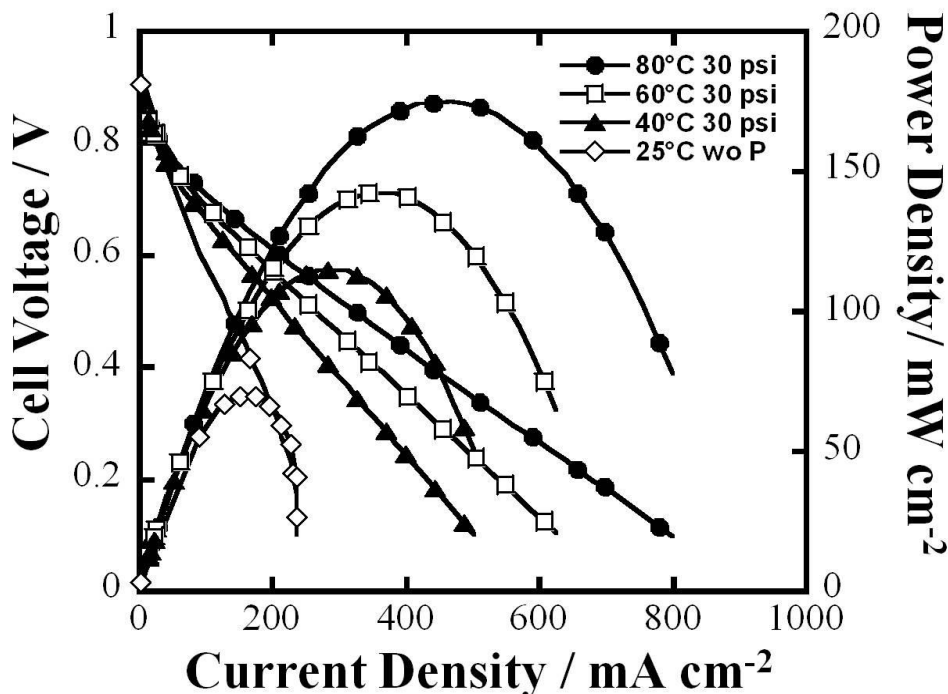


Figure 1. Performance of a single fuel cell of $\text{Ru}_3\text{Pd}_6\text{Pt}$ (40 wt.%)/C with catalyst loading of 0.64 mg cm^{-2} as cathode and Pt(20 wt\%/C) with catalyst loading of 0.8 mg cm^{-2} . Operating with H_2/O_2 at different temperatures from 25°C to 80°C .

4. CONCLUSIONS

The use of the polyol method as a synthetic technique toward the synthesis of a low platinum content catalyst has been demonstrated. Small homogeneous agglomerated particles with spherical shape with less than 100 nm containing crystallites of 3-9 nm in size were determined. The prepared three-metallic catalysts exhibit a high electrocatalytic activity toward the $4e^-$ oxygen reduction reaction and thus could be considered as a cathode material for PEM fuel cells. A performing of 175 mW cm^{-2} was reached at 0.40V and 80°C . The MEA performance would be enhanced by optimizing the electrocatalyst synthesis and the anode and cathode catalyst loading.

ACKNOWLEDGMENTS

We gratefully acknowledge the financial support of the National Council of Science and Technology, CONACYT (grant FOINS-2250-6) and Science and Technology Institute, ICYTDF (grant PICCO 10-3). FLN thanks CONACYT for the doctoral fellowship and Adolfo Tavira for the XRD pattern; Paz del Angél for TEM micrographs and José Romero for the SEM micrographs.

References

1. G. Chaudhuri, S. Paria, *Chem. Rev.*, 112 (2012) 2373.
2. T. Cochell, A. Manthiram, *Langmuir*, 28 (2012) 1579.
3. C.H. Wang, N.M. Markovic, V.R. Stamenkovic, *ACS Cat.*, 2 (2012) 891.
4. M.S. Thorum, J.M. Hankett, A.A. Gewirth, *J. Phys. Chem. Lett.*, 2 (2011) 295.
5. G. Ramos-Sánchez, Mariano M. Bruno, Yohann R. Thomas, Horacio R. Corti, O. Solorza-Feria, *Int. J. Hydrogen Energy*, 37 (2012) 31.
6. A. Godínez-García, J.F. Pérez-Robles, H. Vladimir Martínez-Tejada, O. Solorza-Feria, *Mat. Chem. Phys.*, 134 (2012) 1013.
7. K. Sathish- Kumar, G. Vázquez-Huerta, A. Rodríguez-Castellanos, H. M. Poggi-Varaldo, O. Solorza-Feria, *Int. J. Electrochem. Sci.*, 7 (2012) 5484.
8. A. Munar, K. Suárez, O. Solorza, N.P. Berezina, V. Compañ, *J. Electrochem. Soc.*, 157 (2010) B1186.
9. Y. Wang, K.S. Chen, J. Mishler, S.Ch. Cho, X.C. Adroher, *Appl. Energy*, 88 (2011) 981.
10. H. Zhang, P. K. Shen, *Chem. Rev.*, 112 (2012) 2780.
11. D.C. Martínez-Casillas, G. Vázquez-Huerta, J.F. Pérez-Robles, O. Solorza-Feria, *J. Power Sources*, 196 (2011) 4468.
12. M. Neergat, V. Gunasekar, R. Rahul, *J. Electroanal. Chem.*, 658 (2011) 25.
13. C. Grolleau, C. Coutanceau, F. Pierre, J.M. Leger, *J. Power Sources* 195 (2010) 1569.
14. K. Nagaveni, A. Gayen, G. N. Subbanna, M. S. Hegde, *J. Mater. Chem.*, 12 (2002) 3147.
15. S. Harish, S. Baranton, Ch. Coutanceau, J. Joseph, *J. Power Sources*, 214 (2012) 33.
16. S. M. Durón-Torres, F. Leyva-Noyola, M. Galván-Valencia, O. Solorza-Feria. *J. New Mat. Electrochem. Systems*, 11 (2008) 75.
17. J.J. Salvador-Pascual, V. Collins-Martínez, A. López-Ortiz, O. Solorza-Feria, *J. Power Sources*, 195 (2010) 3374.
18. K. Suárez-Alcántara, O. Solorza-Feria, *Electrochim. Acta*, 53 (2008) 4981.
19. J. Yang, C. H. Cheng, W. Zhou, J. Y. Lee, Z. Liu, *Fuel Cells*, 10 (2010) 907.
20. H. Ye, J.A. Crooks, *Langmuir*, 23 (2007) 11901.
21. A. Cuesta, A. Couto, A. Rincón, M.C. Pérez, A. López, C. Gutiérrez, *J. Electrochem. Chem.*, 586 (2006) 184.

22. A.J. Bard, L. Faulkner. *Electrochemical methods: principles and applications*. New York. Willey, 2001, p. 341.
23. A. Velasco Martínez, M. Torres Rodríguez, M. Gutierrez Arzaluz, P. Angel Vicente, O. Solorza Feria. *Int. J. Electrochem. Sci.*, 7 (2012) 7140.
24. A. Ezeta-Mejía, O. Solorza-Feria, H.J. Dorantes-Rosales, J.M. Hallen López, E.M. Arce Estrada. *Int. J. Electrochem. Sci.*, 7 (2012) 8940.
25. C. Coutanceau, P. Crouigneau, J. M. Leger, C. Lamy. *J. Electroanal. Chem.*, 379 (1994) 389.
26. A. Godínez-García, J.F. Pérez-Robles, H.V. Martínez-Tejeda, O. Solorza-Feria. *Mat. Chem. Phys.*, 134 (2012) 1013.
27. F. Godínez-Salomón, M. Hallen-López, O. Solorza-Feria. *Int. J. Hydrogen Energy*, 37 (2012) 14902.